

P1.54 Advection-Diffusion Equation on Unstructured Adaptive Grids

Nash'at Ahmad* and Zafer Boybeyi

School of Computational Sciences
George Mason University
Fairfax, Virginia

1 INTRODUCTION

Discretizations based on unstructured grids have been widely used in other scientific disciplines for modeling problems bounded by complex geometries. Solution-adaptive techniques are relatively easy to implement on unstructured grids and in addition they provide a convenient way to model the multi-scale spanning nature of atmospheric flows. This paper describes the implementation of a higher-order Godunov-type scheme on unstructured adaptive grids for the advection-diffusion equation in two dimensions. Validation of the numerical scheme and the solution-adaptive technique against exact solutions of benchmark cases is discussed. It is shown that the scheme is conservative, exhibits little numerical diffusion and is well suited for modeling Eulerian transport. The improvement in computational efficiency while maintaining the accuracy of the solution *via* solution-adaptive techniques is also demonstrated.

The unstructured grid technique has been extensively applied in engineering problems for discretizing computational domains with complex geometries (Baum and Löhner 1989; Löhner 2001; Luo et al. 2003). This capability is essential for resolving complex terrain features and shoreline boundaries for mesoscale (Bacon et al. 2000; Boybeyi et al. 2001) and urban-scale modeling (Camelli et al. 2004). In addition, computational efficiency can be achieved by providing variable and continuous resolution throughout the computational domain, with a high mesh resolution only in regions of interest (Ahmad et al. 1998; Behrens et al. 2000; Ghorai et al. 2000; Sarma et al. 1999).

The Eulerian transport model is usually favored when dealing with complex physical processes such as advection of chemically reactive agents or wet deposition. Eulerian approach is also considered to be more suitable for describing diffusion in non-stationary and non-homogeneous flows (Arya 1999). Another advantage is the simplicity of the flow model itself compared to the Lagrangian approach. In spite of these advantages there are also limitations associated with the Eulerian models.

In general, the Eulerian transport models suffer from several limitations. Firstly, the treatment of advection in Eulerian models usually introduces artificial numerical diffusion and sometimes, spurious oscillatory behavior. This can be a problem when advecting non-negative physical quantities such as concentrations. Secondly, use of the gradient-transfer hypothesis limits these models to time scales much larger than the turbulence integral time scale and to pollutant spatial scales much larger than the turbulence integral spatial scales. Thirdly, the pollutant mass being modeled must have a spatial extent that is, at least equal to four or more horizontal and vertical mesh increments in order to adequately define the gradients and minimize advection phase errors. Finally, the above-mentioned limitations make the treatment of point and line sources in Eulerian models particularly difficult.

Eulerian transport models therefore, require both accurate numerical schemes and fine mesh resolution. However, limitations on computational resources can prohibit the use of high mesh resolution throughout the computational domain. Unstructured adaptive grids can be used to minimize the computational overhead while attempting to attain the desirable accuracy in the solution. This paper discusses both the implementation and the validation of a higher-order Godunov-type scheme on unstructured adaptive grids and the use of solution-adaptive techniques to overcome some of the limitations of the Eulerian transport models.

2 NUMERICAL SCHEME

The two-dimensional unsteady advection-diffusion equation in the absence of source terms can be written in the conservative form as:

$$\frac{\partial Q}{\partial t} + \frac{\partial F}{\partial x} + \frac{\partial G}{\partial y} = \frac{\partial}{\partial x} \left(k \frac{\partial Q}{\partial x} \right) + \frac{\partial}{\partial y} \left(k \frac{\partial Q}{\partial y} \right) \quad (1)$$

where,

$$Q = q, \quad F = qu, \quad G = qv \quad (2)$$

q is the Eulerian tracer, k is the diffusion coefficient, u is the velocity component in the x -direction and v is the velocity component in the y -direction. The advection part of the scalar transport equation is solved using a higher-order Godunov-type scheme (Godunov 1959).

* Corresponding author address: Nash'at Ahmad, School of Computational Sciences, MS 5B2, George Mason University, Fairfax, Virginia 22030.

e-mail: nahmad6@gmu.edu

These finite volume discretizations are conservative and have the ability to resolve regions of steep gradients accurately, thus avoiding dispersion or phase errors in the solution. Eqns. (1)-(2) can be written in the integral form as:

$$\frac{d}{dt} \int_{\Omega} Q d\Omega = - \oint_{\Gamma} (F, G) \cdot \bar{n} d\Gamma + \oint_{\Gamma} J \cdot \bar{n} d\Gamma \quad (3)$$

where, $J = -k\nabla Q$, \mathbf{n} is the unit normal pointing out of the control surface Γ of the control volume Ω . Figure 1 shows the cell-centered control volume, Ω with each of its control surfaces and the unit normals pointing outwards from the control surfaces. Eqn. (3) can be approximated directly:

$$V_{cell} \frac{dQ_{cell}}{dt} + \sum_{faces} (F, G) \cdot s = \sum_{faces} (J) \cdot s \quad (4)$$

where, V_{cell} is the volume of the control volume (area of the triangle in the case of the two-dimensional triangular mesh), Q_{cell} is the cell-averaged value of the conserved quantity Q at cell center and s is the control surface area (edge lengths of the triangle in case of the two-dimensional mesh).

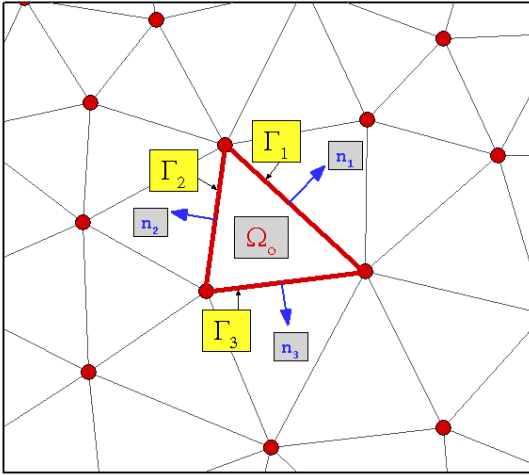


Figure 1: Control volume Ω_0 .

The fluxes are calculated by summing all the incoming and outgoing fluxes through each face of the control volume. As mentioned earlier, the advective flux across each edge of the cell is calculated using Godunov's method. The values on either side of a cell edge form the initial conditions for the Riemann problem (for details see Toro 1999). The solution is marched in time within the multi-stage Runge-Kutta explicit time marching scheme (Jameson et al. 1981). In a loop over edges the values of cells on either side of the edge are used to calculate the fluxes. Once the fluxes have been calculated, they are added to the cell centered value in

a loop over cells. For the higher-order calculation gradient-limited extrapolated values are used in the Riemann solver instead of cell averages (van Leer 1979). Both the Green-Gauss and the Linear Least-Squares gradient reconstruction (Barth and Jespersen 1989) techniques have been implemented to extend the spatial accuracy of scheme to higher-order. The scheme is made *total variation diminishing* (Harten 1983) with the help of slope limiters (Barth and Jespersen 1989; van Leer 1979). The diffusive flux across the edge is calculated by finding the gradients on the edge:

$$J = k \left(\frac{\partial q}{\partial x} \right)_{face} n_x + k \left(\frac{\partial q}{\partial y} \right)_{face} n_y \quad (5)$$

where, k is the diffusion coefficient and n_x and n_y are the edge normal unit vectors in x and y -directions respectively. In practice, unstructured meshes do not have an orthogonal structure (the line intersecting the cell centers on either side of an edge would be perpendicular to the edge for an orthogonal mesh, e.g., a mesh consisting of only equilateral triangles). Therefore, a correction term is included to account for this lack of orthogonality:

$$\left(\frac{\partial q}{\partial x} \right)_{face} = \left(\frac{\partial q}{\partial x} \right)_{ave} - \frac{\partial q}{\partial c} c_x \quad (6)$$

$$\left(\frac{\partial q}{\partial y} \right)_{face} = \left(\frac{\partial q}{\partial y} \right)_{ave} - \frac{\partial q}{\partial c} c_y \quad (7)$$

where, c denotes the line connecting cell centers on either side of an edge (line connecting points (x_{il}, y_{il}) and (x_{ir}, y_{ir}) in Figure 2) and c_x and c_y are the normal unit vectors for the line segment c . The correction term is given by:

$$\frac{\partial q}{\partial c} = \left(\frac{\partial q}{\partial x} \right)_{ave} c_x + \left(\frac{\partial q}{\partial y} \right)_{ave} c_y - \frac{q_{il} - q_{ir}}{\bar{c}} \quad (8)$$

q_{il} and q_{ir} are the scalar quantities in the cell to the left and the right of the edge and \bar{c} is the length of the line connecting the cell centers on the either side of the edge. The average gradient on the cell faces is calculated by a simple average of gradients in the cells on either side of the edge (in cells il and ir):

$$\left(\frac{\partial q}{\partial x} \right)_{ave} = 0.5 \left(\left(\frac{\partial q}{\partial x} \right)_{il} + \left(\frac{\partial q}{\partial x} \right)_{ir} \right) \quad (9)$$

$$\left(\frac{\partial q}{\partial y} \right)_{ave} = 0.5 \left(\left(\frac{\partial q}{\partial y} \right)_{il} + \left(\frac{\partial q}{\partial y} \right)_{ir} \right) \quad (10)$$

The cell-centered value of the gradients is also needed in the extrapolation for the higher-order advection scheme and is calculated using the methods mentioned earlier. The time step restriction due to advection is given by:

$$\Delta t(\text{advection}) = CFL \frac{\Delta x}{\text{abs}(u)} \quad (11)$$

where, u is the normal velocity at edge and Δx is the distance between the cell center and the point of intersection of the edge with the line connecting the cell centers on either sides of the edge (see Figure 2). The CFL criteria was set to 0.9 in all simulations. The time step restriction due to diffusion is given by:

$$\Delta t(\text{diffusion}) = \frac{\Delta x^2}{4k} \quad (12)$$

Since, the time step due to diffusion is too restrictive, both explicit and implicit time-marching schemes have been implemented.

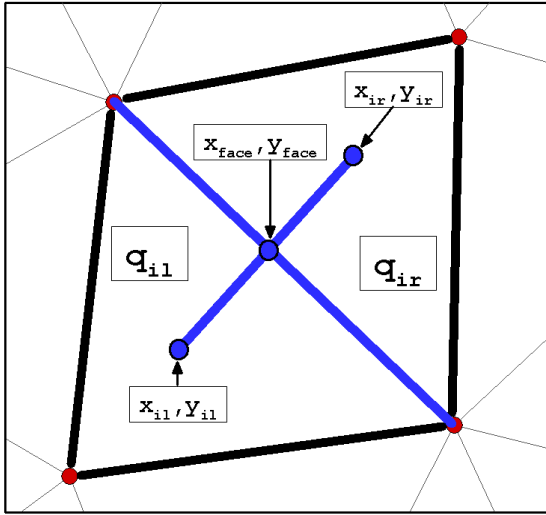


Figure 2: Calculation of diffusive fluxes.

The methodology used for dynamically adapting the mesh is described in Ahmad et al. (1998).

3 RESULTS

The results from three analytical test cases are discussed in this section. A convergence study to measure the order of accuracy of the flow solver (advection equation), a solution-adaptive simulation to demonstrate the advantage of using unstructured grids (advection equation) and finally the advection-diffusion equation was simulated for validation against exact solution.

3.1 Convergence Study

The simulation of Doswell's cyclogenesis problem (Doswell 1984) is presented in this section. A convergence study was performed to observe the reduction in error with increased mesh resolution and the cost of higher accuracy, which comes with it. The scalar advection equation was solved for this case. The flow field for the Doswell test can be defined as follows:

$$u(x, y) = -\frac{y}{r} \frac{f_t}{f_{\max}}; \quad v(x, y) = \frac{x}{r} \frac{f_t}{f_{\max}} \quad (13)$$

where, r is the distance from any given point to the origin of the coordinate system (i.e. the point: $x = 0$ and $y = 0$), $f_{\max} = 0.385$ is the maximum tangential velocity and f_t is given by:

$$f_t = \frac{\tanh(r)}{\cosh^2(r)}. \quad (14)$$

The simulation was run for $t = 4$ units. The evolution of tracer field in time t , is given by the exact solution:

$$q(x, y, t) = -\tanh\left[\frac{y}{\delta} \cos(f \cdot t) - \frac{x}{\delta} \sin(f \cdot t)\right], \quad (15)$$

$$f = \frac{1}{r} \frac{f_t}{f_{\max}}. \quad (16)$$

where, δ is the characteristic width of the frontal zone. The value of δ was set to 2 for a smooth cyclogenesis. The initial tracer field can be obtained from Eqn. (15) by setting $t = 0$. Error in the solution is defined in terms of the L_2 -norm (Burg et al. 2002):

$$E_{L2} = \sqrt{\sum_{i=1}^{\text{cells}} (q_i^{\text{exact}} - q_i^{\text{computed}})^2 A_i} \quad (17)$$

where, A_i is the area of each cell/element. The edge lengths of even a fairly uniform unstructured mesh can vary and all the triangles are usually not equilateral for a good quality smooth mesh. To circumvent these issues, a triangular mesh was generated and then each triangle was subdivided into 4 triangles. The resulting meshes consist of only equilateral triangles and at each successive refinement step the mesh resolution is exactly doubled. The order of accuracy, p of a numerical scheme can be obtained from:

$$p \approx \frac{1}{\ln(2)} \ln\left(\frac{E^{2h}}{E^h}\right) \quad (18)$$

where, E^{2h}/E^h is the ratio of error between meshes of resolutions h and $2h$. The average order of accuracy obtained from the test was 2.05. Table 1 lists some of the parameters of the three meshes used in the study and Figure 3 shows an intermediate mesh for the triangular domain. The mesh shown has 1024 cells. One refinement step on it will result in Mesh 1. The computed solution on Mesh 2 is shown in Figure 4. Figure 5 shows the reduction in error as the mesh resolution is increased and the associated computational cost is shown in Figure 6. It is clear that given a finite amount of resources, a global refinement of the mesh may not be a feasible way to improve the solution accuracy. One way to achieve computational efficiency would be to use solution-adaptive techniques.

Table 1: Grids used in the convergence study.

mesh	Δx	cells
1	0.1804	4096
2	0.0902	16384
3	0.0451	65536

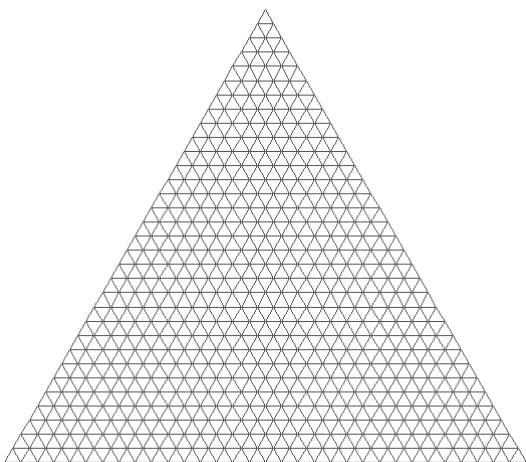


Figure 3: An intermediate mesh.

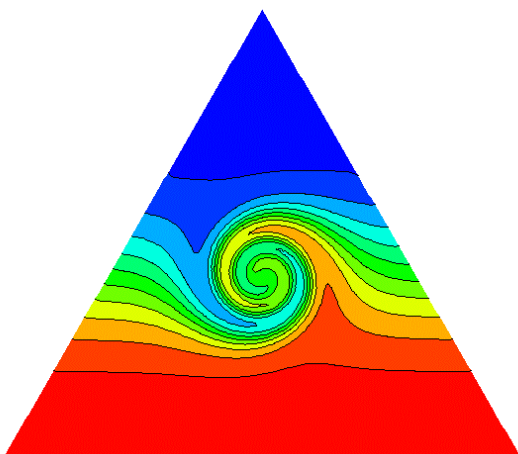


Figure 4: Computed solution on Mesh 2.

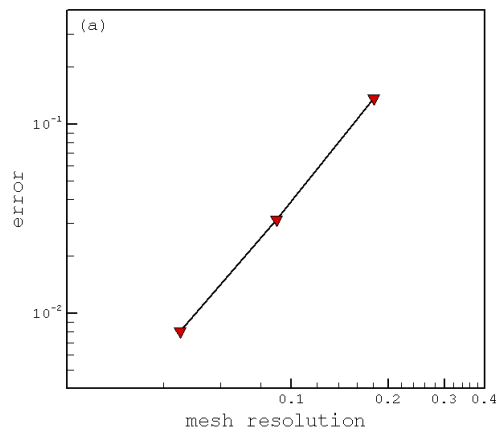


Figure 5: Error vs. Δx .

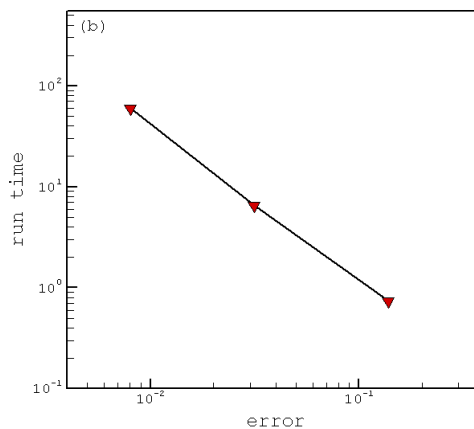


Figure 6: Run-time vs. error.

3.2 Solution-Adaptation

The basic idea behind adaptive mesh refinement is to distribute the error equally over a computational mesh. The regions, where numerical error is large, are refined to provide greater spatial accuracy. In the current study, adaptation was achieved via h -refinement in which, the conservation of quantities is easier to maintain during interpolation and computational overhead is also smaller compared to, *e.g.*, re-meshing.

If the exact solution is known then the error-indicator (adaptation criteria) can easily be defined in terms of relative error or a similar quantity. In practice the exact solution is not known *a priori*. The regions of large errors however usually coincide with regions of high gradients. There are various ways in which one can define the adaptation criteria (Ahmad et al. 1998; Löhner 2001; Ghorai et al. 2000; Gopalakrishnan et al. 2002) depending on the problem. Ahmad et al. (1998) tag cells for refinement based on a Gaussian function around Lagrangian particles (for atmospheric dispersion simulations). The adaptation criteria proposed by Löhner (2001) is a function of the Laplacian, first derivatives and differences (for tracking shock wave

propagation, fluid-structure interactions, etc.). Ghorai et al. (2000) have based their error-indicator on the difference between the first and second-order solutions (for Eulerian transport and diffusion simulations).

In the current study a simple error-indicator was used. Three radii were defined – R_{con} was set to the radius of the cone; R_{ref} was 2 units larger than R_{con} and R_{cor} was defined as 4 units larger than R_{con} (see Figure 7). The maximum and minimum allowable edge lengths were also specified. The cells were tagged for refinement if a cell with large edge lengths was found between R_{con} and R_{ref} and cells were tagged for deletion if a cell with small edge lengths was found outside the circle defined by R_{cor} . The refinement cycle was invoked every 15 iterations and the coarsening cycle was invoked every 150 iterations.

The adaptation criteria used in this study is simple, but has direct relevance to dispersion modeling. An area of influence, e.g., can be defined around the puff centers as the adaptation criteria.

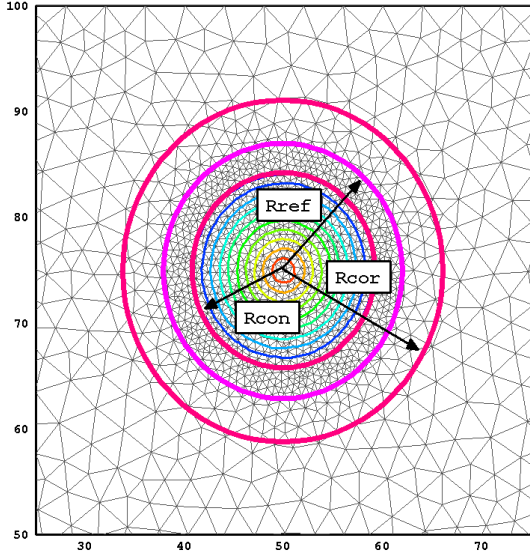


Figure 7: Rotating Cone Test. Adaptation criteria.

The domain was bounded within $[0,100] \times [0,100]$. The cone was centered at $(x_o, y_o) = (50, 75)$ with a radius of 10 units. The rotational flow field was defined as follows:

$$u(x, y) = -\omega(y - y_o) \quad (19)$$

$$v(x, y) = \omega(x - x_o) \quad (20)$$

where, $u(x, y)$ and $v(x, y)$ are the velocities in the x and y -direction respectively, $\omega = 0.4$ is the constant angular velocity and $(x_o, y_o) = (50, 50)$ is the center of the mesh. The simulation was run for 15.7079 s (time taken by the cone to complete one revolution = $2\pi/\omega$). The unstructured mesh was defined in terms of boundary

edges (100 edges on each side for the globally refined mesh and 25 edges on each side for the adaptive mesh). The adaptive mesh started with a minimum edge length of 0.337 and a maximum edge length of 4.667. Some of the mesh parameters are listed in Table 2. The boundary conditions are defined with the help of *ghost* cells (LeVeque 2002), which are mirrors of the boundary cells. Transmissive boundary conditions (LeVeque 2002) were used in the calculations.

Figure 8 shows the initial concentration contours, tracer field at an intermediate stage and after one revolution for the solution-adaptive run. Errors and timings for the solution-adaptive run and the simulation on a globally refined mesh are tabulated in Table 2. The timing was obtained by using the Linux *time* command. Calculations were made on a P4 Dell Laptop running RedHat Linux 7.3. The phase error was defined as follows (Iselin et al. 2002):

$$E_{phase} = \sqrt{(x^{exact} - x^{comp})^2 + (y^{exact} - y^{comp})^2} \quad (21)$$

where, x^{exact} and y^{exact} are the coordinates of cell in which the tracer *maxima* lies for the exact solution and x^{comp} and y^{comp} are the coordinates of the cell in which the *maxima* lies for the computed solution. The diffusion error was found by subtracting the computed tracer *maxima* from the exact value of the tracer *maxima* (Iselin et al. 2002):

$$E_{diffusion} = \max(q^{exact}) - \max(q^{comp}) \quad (22)$$

Table 2: Rotating Cone Tests

	fine	adaptive
E_{L2}	0.35297	0.79073
E_{phase}	0.29900	0.56245
$E_{diffusion}$	0.13924	0.16537
real time	~130 min	~35 min
max edge	1.27941	4.93815
min edge	0.21593	0.22007
$n_{cells}_{initial}$	48366	4830
n_{cells}_{final}	48366	7872

The adaptive mesh reproduces comparable results to the globally refined mesh at a reduced computational cost (adaptive run is approximately 4 times faster). It should be noted that the code used to generate the results is still under development and is more of a research tool currently. A further reduction in timing may be achieved by code optimization. The comparison of the computed tracer field on the adaptive mesh and the globally refined mesh with the exact solution is shown in Figure 9. The figure shows concentration profiles at $y = 75$ for x between 25 and 75. The adaptive run is slightly more diffusive than the run on the globally refined mesh.

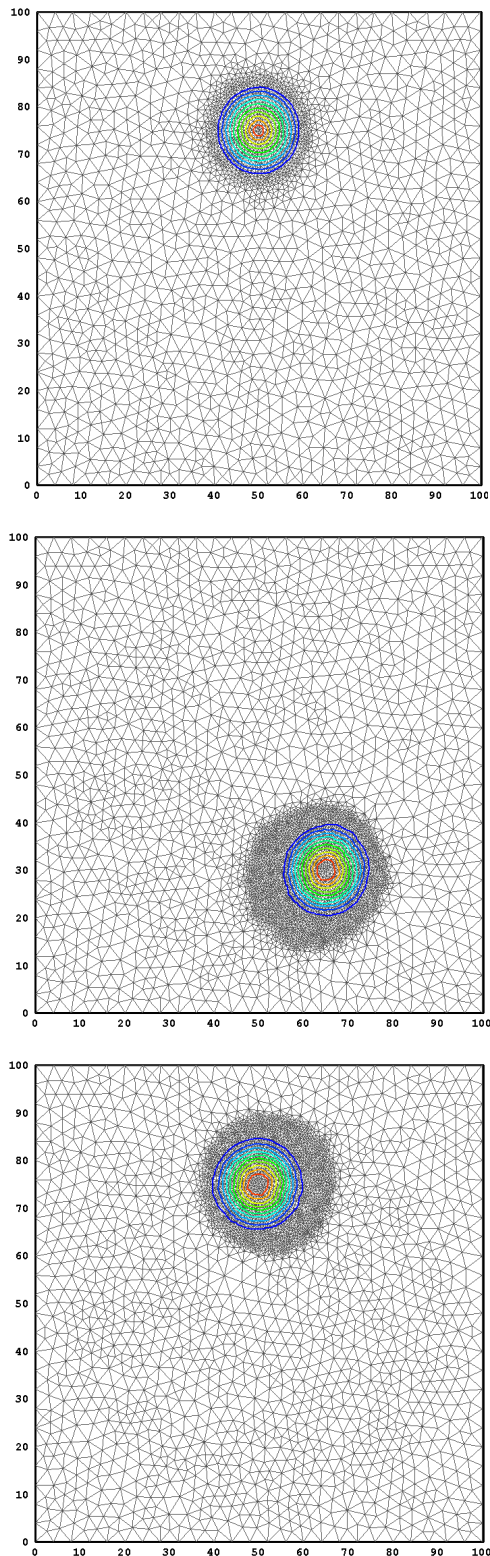


Figure 8: Rotating Cone Test. Initial conditions (top); at an intermediate stage (middle) and after one complete revolution (bottom).

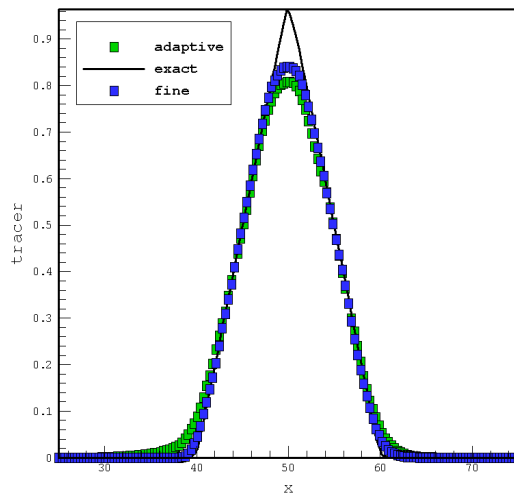


Figure 9: Rotating Cone Test. Comparison with exact solution.

3.3 Advection-Diffusion

In this section the results of the test case for the advection-diffusion equation proposed by Noye and Tan (1989) are presented. The test case describes the diffusion of an initial Gaussian pulse as it is advected along a straight line. The domain was bounded within $[0,2] \times [0,2]$. The mesh was defined in terms of boundary edges (100 edges on each side of the computational domain). The resulting mesh consisted of 39386 cells. The analytical solution of the unsteady advection-diffusion for the Noye-Tan test case is given by:

$$q(x, y, t) = \frac{1}{4t+1} \exp \left[-\frac{(x-ut-x_o)^2}{k_x(4t+1)} - \frac{(y-vt-y_o)^2}{k_y(4t+1)} \right] \quad (23)$$

where, $k_x = k_y = 0.01$ are the diffusion coefficients and $u = v = 0.8$ are the velocities in the x - and y -direction respectively. $x_o = y_o = 0.5$ is the center of the initial tracer distribution. The initial conditions and the Dirichlet boundary conditions can be obtained from the analytical solution by setting $t = 0$. The simulation was ran for $t = 1.25$. The initial conditions and the computed solution at $t = 1.25$ are shown in Figure 10. A comparison between the exact solution and the computed solution along the mesh diagonal is shown in Figure 11. The computed solution matches well with the exact solution in the current study. Solution-adaptation was not used in this simulation.

In this test case no source terms are included which simplifies the problem. Validations against cases that include the source terms (analytical cases as well as experimental data) will have to be conducted to further verify the robustness of the flow solver.

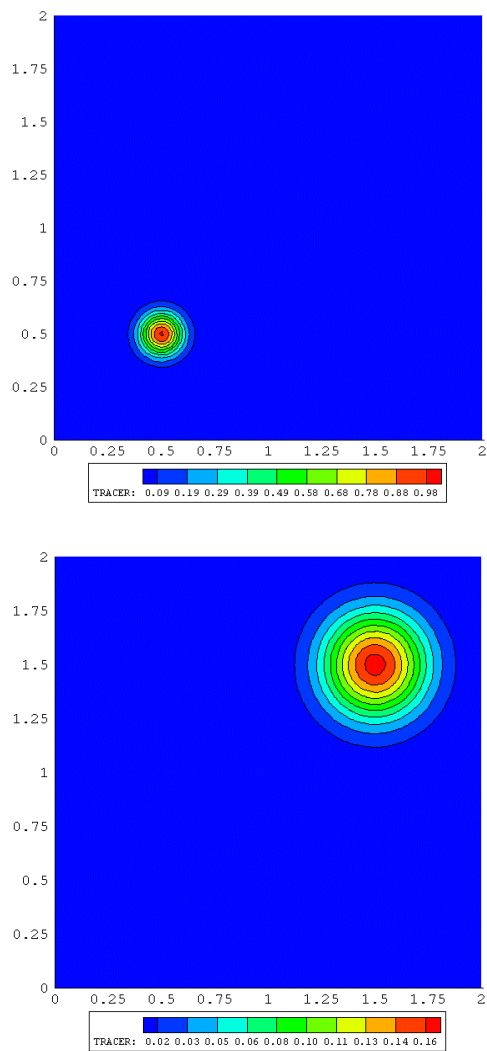


Figure 10: Noye-Tan Test. Initial conditions (top) and solution at $t=1.25$ (bottom).

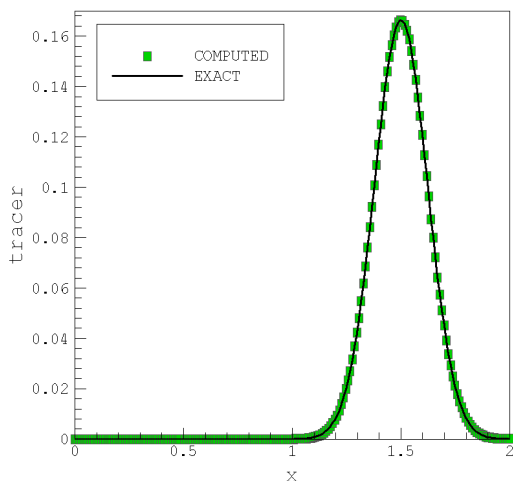


Figure 11: Comparison between the exact solution and the computed solution along the mesh diagonal.

4 CONCLUSIONS

A higher-order Godunov-type scheme was applied to model Eulerian transport on unstructured grids. The method was validated against analytical solutions for different benchmark cases and the results are encouraging. The scheme is conservative and exhibits minimal numerical diffusion and dispersion errors. It was also shown that the solution-adaptive technique improves the computational efficiency while maintaining the fidelity of the solution.

REFERENCES

Ahmad, N., D. Bacon, Z. Boybeyi, T. Dunn, M. Hall, P. Lee, D. Mays, A. Sarma and M. Turner, 1998: A Solution-Adaptive Grid Generation Scheme for Atmospheric Flow Simulations. *Numerical Grid Generation in Computational Field Simulations*, Proceedings of the 6th International Conference held at University of Greenwich. pp. 327-335.

Arya, P., 1999: *Air Pollution Meteorology and Dispersion*. Oxford University Press. 310 pp.

Bacon, D. P., N. N. Ahmad, Z. Boybeyi, T. J. Dunn, M. S. Hall, P. C. S. Lee, R. A. Sarma, M. D. Turner, K. Waight, S. Young, and J. Zack, 2000: A Dynamically Adapting Weather and Dispersion Model: The Operational Multiscale Environment Model with Grid Adaptivity (OMEGA). *Mon. Wea. Rev.*, **128**, 2044-2076.

Barth, T. J., and D. C. Jespersen, 1989: The Design and Application of Upwind Schemes on Unstructured Meshes. AIAA Paper 1989-0366.

Baum, J. D., and R. Löhner, 1989: Numerical Simulation of Shock-Elevated Box Interaction Using an Adaptive Finite Element Shock Capturing Scheme. AIAA Paper 1989-0653.

Behrens, J., K. Dethloff, W. Hiller, and A. Rinke, 2000: Evolution of Small-Scale Filaments in an Adaptive Advection Model for Idealized Tracer Transport. *Mon. Wea. Rev.*, **128**, 2976-2982.

Boybeyi, Z., N. Ahmad, D. Bacon, T. Dunn, M. Hall, P. Lee, A. Sarma and T. Wait, 2001: Evaluation of the Operational Multiscale Environment Model with Grid Adaptivity against the European Tracer Experiment. *J. App. Met.* **40**. 1541-1558.

Burg, C., K. Sreenivas, D. Hyams, and B. Mitchell, 2002: Unstructured Nonlinear Free Surface Flow Simulations: Validation and Verification. AIAA Paper 2002-2977.

Doswell, C. A., 1984: A Kinematic Analysis of Frontogenesis Associated with a Nondivergent Vortex. *J. Atmos. Sci.*, **41**, 1242-1248.

Camelli, F., R. Löhner, W. C. Sandberg and R. Ramamurti, 2004: VLES Study of Ship Stack Gas Dynamics. AIAA Paper 2004-0072.

- Ghorai, S., A. S. Tomlin, and M. Berzins, 2000: Resolution of pollutant concentrations in the boundary layer using a fully 3D adaptive gridding technique. *Atmospheric Environment* **34**, 2851-2863.
- Godunov, S. K., 1959: A Finite Difference Method for the Computation of Discontinuous Solutions of the Equations of Fluid Dynamics. *Mat. Sb.*, **47**, 357-393.
- Gopalakrishnan, S. G., D. Bacon, N. Ahmad, Z. Boybeyi, T. Dunn, M. Hall, P. Lee, R. Madala, A. Sarma, M. Turner, and T. Wait: 2002: An Operational Multiscale Hurricane Forecasting System. *Mon. Wea. Rev.*, **130**, 1830-1847.
- Harten, A., 1983: High resolution schemes for hyperbolic conservation laws. *J. Comp. Phys.*, **49**, 357-393.
- Iselin, J., J. M. Prusa and W. J. Gutowski, 2002: Dynamic Grid Adaptation Using MPDATA Scheme. *Mon. Wea. Rev.*, **130**, 1026-1039.
- Jameson, A., W. Schmidt, and E. Turkel, 1981: Numerical Solution of the Euler Equations by Finite Volume Method using Runge-Kutta Time Stepping Schemes. AIAA Paper 1981-1259.
- LeVeque, R. J., 2002: *Finite Volume Methods for Hyperbolic Problems*. Cambridge University Press. 558 pp.
- Löhner, R., 2001: *Applied CFD Techniques: An Introduction based on Finite Element Methods*. John Wiley and Sons Ltd. 366 pp.
- Luo, H., J. D. Baum, and R. Löhner, 2003: Extension of HLLC Scheme for Flows at all Speeds. AIAA Paper 2003-3840.
- Noye, B. J., and H. H. Tan, 1989: Finite difference methods for solving the two-dimensional convection-diffusion equation. *Int. J. Num. Methods Fluids*, **9**, 75-98.
- Sarma, A., N. Ahmad, D. Bacon, Z. Boybeyi, T. Dunn, M. Hall and P. Lee, 1999: Application of Adaptive Grid Refinement to Plume Modeling. *Air Pollution VII*. WIT Press. 59-68.
- Toro, E. F., 1999: *Riemann Solvers and Numerical Methods for Fluid Dynamics*. Springer-Verlag. 624 pp.
- van Leer, B., 1979: Towards the Ultimate Conservative Difference Scheme. V. A Second-Order Sequel to Godunov's Method. *J. Comp. Phys.*, **32**, 101-136.